REVIEW

Review on reactive species in water treatment using electrical discharge plasma: formation, measurement, mechanisms and mass transfer

Plasma Sci. Technol. **20** (2018) 103001 (17pp) https://doi.org/10.1088/2058-6272/aacff4

Review

Review on reactive species in water treatment using electrical discharge plasma: formation, measurement, mechanisms and mass transfer

Yang CAO (曹洋)[1,2], Guangzhou QU (屈广周)[1,2], Tengfei LI (李腾飞)[1,2], Nan JIANG (姜楠)[3] and Tiecheng WANG (王铁成)[1,2]

[1] College of Natural Resources and Environment, Northwest A&F University, Yangling 712100, People's Republic of China
[2] Key Laboratory of Plant Nutrition and the Agri-environment in Northwest China, Ministry of Agriculture, Yangling 712100, People's Republic of China
[3] Institute of Electrostatics and Special Power, Dalian University of Technology, Dalian 116024, People's Republic of China

E-mail: wangtiecheng2008@126.com

Received 20 March 2018, revised 19 June 2018
Accepted for publication 25 June 2018
Published 20 August 2018

Abstract

In the electrical discharge plasma process, various chemical and physical processes can participate in the removal of contaminants. In this paper, the chemical and physical processes that occur as a result of the electrical discharge plasma are reviewed, and their possible roles in the degradation of contaminants are discussed. Measurement methods for the quantification of important reactive species and their advantages and shortcomings are presented. Approaches on how to enhance the diffusion of the reactive species in solution are examined. In addition, the formation of typical reactive species in different electrical discharge plasma is compared.

Keywords: advanced oxidation process, electrical discharge plasma, reactive species, wastewater treatment

(Some figures may appear in colour only in the online journal)

1. Introduction

The international and national regulations on the discharge of various contaminants into the aquatic environment from wastewater treatment plants are becoming increasingly strict. Many of these contaminants are hazardous and toxic to the environment and human health. Thus, it is urgent to remove these hazardous and toxic contaminants from wastewater via various methods. Conventional processes involved in wastewater treatment can be categorized as biological, physical, and chemical methods [1, 2].

Biological processes are the most widely applicable treatment processes for wastewater because of their low costs. However, traditional biological processes are unable to effectively treat wastewater containing some non-biodegradable and biocidal compounds; and the treatment processes are quite slow and require the maintenance of rigorous conditions for the growth of microorganisms [1, 2]. Generally, physical treatment processes only separate the undesirable components from wastewater by several means; they achieve only the phase transfer of contaminants, allowing the contaminants to remain in the environment [2]. Conventional chemical treatment processes are

employed to treat industrial wastewater and groundwater by using oxidative chemicals, such as ClO_2, Cl_2, H_2O_2, O_3, and $KMnO_4$. However, the relatively high cost of such chemical treatment processes and the risks of secondary pollution due to the usage of some chemicals limit their wide applications [3, 4].

Advanced oxidation processes (AOPs) have drawn considerable interest in water treatment because of the generation of ·OH in the treatment process; ·OH is a strong oxidant, and it can rapidly oxidize various organic compounds in wastewater [4–8]. Among the AOPs, electrical discharge plasma is widely employed for wastewater treatment. When the electrical discharge plasma is triggered, both physical and chemical effects are involved; the physical effects include ultraviolet (UV) radiation, shock waves, cavitation effects, and high temperature pyrolysis; while the chemical effects involve the formation of reactive species and oxidation of organic contaminants [8–20]. All these physical and chemical effects play significant roles in the decomposition of organic contaminants. The advantages of the electrical discharge plasma for wastewater treatment can be summarized as follows: (1) the process can generate lots of highly reactive species, such as H_2O_2, O_3 and ·OH, directly in the liquid phase, and therefore, it does not need to supply external chemicals; (2) the amounts of several reactive species can be conveniently controlled by adjusting the discharge voltage and other process parameters; (3) organic contaminants can be degraded more rapidly and efficiently than by traditional methods due to synergistic actions among the physical and chemical reactions; and (4) the process can be combined with several other processes, such as adsorption and catalytic methods. However, there are still some issues or questions regarding the utilization of electrical discharge plasma in the removal of contaminants, such as the limited information on the possible roles of various physical and chemical effects in contaminant removal, how to accurately measure the amounts of various reactive species and how to optimally utilize them to remove contaminants, and how to effectively enhance the diffusion of the reactive species in the liquid phase to maximize the degradation rates of target contaminants and enhance process efficiency.

Therefore, this paper reviews literature on the physical processes and chemical reactions involved in the electrical discharge plasma process, methods for the quantification of chemically reactive species and the elucidation of their roles, and approaches on how to improve the mass transfer of reactive species to enhance the kinetics of degradation/removal of contaminants in water.

2. Reactions of the electrical discharge plasma

During contaminant removal by electrical discharge plasma, the contaminant degradation processes involved include physical effects and chemical effects. Both the physical and chemical effects are significant in promoting desirable chemical reactions. Contaminants can be decomposed by several physical effects, as well as via chemical reactions with oxidizing species such as O_3, ·O and ·OH.

2.1. Reactions of physical processes

The generation of physical processes involves bubble formation and development [5–7], UV radiation [8–10], cavitation effects and supercritical oxidation [11, 12], high temperature pyrolysis [12], shock waves [13, 14], and electric field effects [15–17]. Bubble formation is mainly involved in the liquid–gas phase discharge plasma process, in which bubbles form when the carrier gas passes through the hollow needle of high-voltage electrodes (the tip of the sharp is 0.2–0.3 mm, and the diameter of the body is 0.7–1.2 mm). Bubbles can also form based on the theory of thermal bubble formation; in this thermal theory, the heat generated by an electric field can produce bubbles, and then the electric field can propagate through the bubbles in a manner similar to that observed in the gas phase [21]. In the presence of gas bubbles, preexisting current resulting from the electron avalanche can heat the surrounding water, and then low density regions can be formed for discharge plasma initiation and propagation. Therefore, discharge plasma can be triggered much more easily in the presence of gas bubbles because a much lower initiation voltage is needed compared with direct liquid phase discharge [6]. Generally, a strong electric field (approximately 10^9 V m^{-1}) is necessary to initiate liquid phase discharge, while about 10^6 V m^{-1} is enough to realize gas phase discharge [22]. Discharge in liquid in the presence of bubbles is an effective pathway for reactive species formation, which can enhance the diffusion of reactive species into the solution, benefiting contaminant degradation.

UV radiation is one of the main forms of discharge power dissipated from electrical discharge in water [8–10]. Generally, the UV radiation from atmospheric pressure gas phase discharges is weaker than that from liquid phase discharges. The types of UV radiation from atmospheric pressure gas phase discharges usually fall within the UVA region with wavelength of 320–400 nm and UVB with wavelength of 280–320 nm; whereas vacuum ultraviolet (VUV, 100–280 nm) can be formed in discharge plasmas in direct contact with water [23]. VUV irradiation efficiently induces chemical reactions because the absorption of VUV by water molecules is large. For example, the absorption of VUV by water containing dissolved oxygen can result in the dissociation of water and O_2, and then ·OH, hydrated electrons, and ·O can be generated. UV radiation can induce chemical reactions with lots of organic pollutants, nitrates and nitrites after penetrating into aqueous solution, as shown in reactions (1)–(5) [24]. In addition, UV radiation can activate some contaminants, resulting in the breakage of the contaminants' molecular bonds, and finally lead to their degradation. Sun [18] reported that there existed an optimum peak pulsed discharge voltage to achieve the strongest UV radiation, and approximately 3.2% of the input energy was released as UV radiation. It was reported that UV radiation was able to contribute to more than 10% of phenol decomposition in a pulsed discharge plasma system [19]. Mok [20] found that the contribution of the UV radiation generated in a dielectric barrier discharge plasma system applied to a wastewater decoloration process was approximately 42%. The UV

radiation effect during a discharge plasma process was investigated by Robinson [25], who reported that approximately 28% of the discharge energy was transformed into UV radiation; in that study, the stored capacitor energy was 1500 J, and 420 J was converted to UV radiation with a peak radiant power of 200 MW. Lukes and co-workers [26] found that increasing the electroconductivity of the solution could increase the flux of UV radiation. Matsumoto *et al* [27] reported that UV radiation played significant roles in bacteria inactivation. Moreover, UV radiation was also generated in the gas phase discharge plasma process (above the water surface) [28]. In our study, we also found that UV radiation contributed to methyl red decoloration in a gas phase surface discharge plasma system [29].

$$h\nu + H_2O \rightarrow \cdot H + \cdot OH, \quad (1)$$

$$h\nu + H_2O \rightarrow H_2 + O, \quad (2)$$

$$h\nu + NO_2^- \rightarrow \cdot NO + \cdot O^-, \quad (3)$$

$$h\nu + NO_3^- \rightarrow \cdot NO_2 + \cdot O^-, \quad (4)$$

$$h\nu + NO_3^- \rightarrow NO_2^- + \cdot O. \quad (5)$$

Supercritical oxidation and cavitation effects are both important physical processes during aqueous discharge plasma, and they can participate in the organic contaminants degradation process. Zhang *et al* [11] reported that supercritical oxidation was one of the significant effects in the aqueous discharge plasma process. Shi *et al* [12] found that approximately 68% of *p*-nitrophenol degradation efficiency could be attributed to the high temperature pyrolysis initiated by supersonic cavitation effects. One important mechanism derived from high temperature pyrolysis is the generation of ·OH in a core high temperature region, as shown in reaction (6), after which a series of other chemical reactions are triggered [30].

$$M + H_2O \xrightarrow{\text{thermal}} \cdot H + \cdot OH + M. \quad (6)$$

In the aqueous discharge plasma process, shock waves with intensity of several MPa occur because of the rapid extension of discharge plasma channels, after which pyrolytic and radical reactions can be initiated [31]. Martin reported that strong shock waves with intensity of 5–20 kbar or 10–20 MPa were generated in a pulsed arc discharge system due to the rapidly expanding plasma channel (1–2 ms) [32]. The detailed characteristics of the shock waves during discharge plasma process were studied by Lu [33], who reported that increasing the discharge voltage could strengthen the shock waves. In addition, the velocity of the shock waves could reach approximately 1.5 km s^{-1} at a discharge voltage of 10 kV, capacitance of 4.1 μF, and electrode distance of 7 mm; and the shock wave pressure in plasma channels was approximately 49 MPa [34]. The shock waves in electrical discharge plasma are mainly utilized in bacteria inactivation and algae removal. Sunka *et al* [35] found that red blood cells could be effectively damaged by shock waves. They also found that the internal structure of a potato (6 cm thickness) was destroyed by shock waves, whereas no injury was observed at the outer surface of the potato [35]. A much greater disinfection efficacy was observed for *Pseudomonas putida* bacteria treated by shock waves than by traditional UV radiation [36].

When an electrical discharge does not form, pulsed high-voltage electric field is an effective method for biological cell disruption and food purification. Electromechanical compression is the main principle driving biological membrane disruption by a pulsed electric field [37]. Lots of transmembrane pores may be formed at a high electric field; the membrane can not repair perturbations when the ratio of total pore area to total membrane area is unfavorable, and then irreversible disruption occurs [38]. Previous research reported that a strong electric field can inactivate microorganisms and remove biofilms on the wall of cooling and drinking water pipes [15–17]. Mizuno and Hori [39] reported that a pulsed high-voltage electric field could rapidly inactivate living cells. In addition, high electric field can also affect chemical reactions in the liquid phase. Hong and Noolandi developed a time-dependent Smoluchowski equation with an electric field, which was helpful for the analysis of the recombination, neutralization, and scavenging processes that occur in the liquid phase [40]. Kuskova described the reaction rate constant in highly polar liquids using the following equation (equation (7)); where E is the electric field, k is Boltzmann's constant, ε is the dielectric permittivity, and T is the absolute temperature. This equation can be used to consider the influences of an electric field on chemical reactions in a liquid phase corona discharge system [41].

$$k(E) = K(0)\exp\left(\frac{2\sqrt{e^3E/\varepsilon}}{kT}\right). \quad (7)$$

2.2. Reactions of chemical processes

Chemical processes in electrical discharge plasma mainly involve chemical reactions of various reactive species (H_2O_2, O_3, ·OH, and ·O, etc). These chemically reactive species are primarily initiated by the attack of high energy electrons. The detailed reaction processes of these reactive species are discussed as follows.

2.2.1. Reactions of high energy electrons. Electrons are generated in the electrical discharge plasma process; the energy of such electrons is able to surpass the dissociation or ionization energy of water molecules [42, 43]. Consequently, the dissociation or ionization of water molecules can occur via electron collisions, resulting in the formation of ·H, ·OH and other hydrated cations [42–44]:

$$e^{-*} + H_2O \rightarrow \cdot OH + \cdot H + e^-, \quad (8)$$

$$e^{-*} + H_2O \rightarrow H_2O^+ + 2e^-, \quad (9)$$

$$H_2O^+ + H_2O \rightarrow H_3O^+ + \cdot OH, \quad (10)$$

where * indicates a high-energy electron state. These generated radicals can then react with each other to form other reactive species, as presented in the following reactions [43, 44]:

$$H + H \rightarrow H_2, \quad (11)$$

$$2 \cdot OH \rightarrow H_2O_2, \quad (12)$$

$$\cdot OH + \cdot H \rightarrow H_2O, \quad (13)$$

$$O_2 + e \rightarrow e + 2 \cdot O, \quad (14)$$

$$O_2 + e^* + M \rightarrow O_2^- + M, \quad (15)$$

$$e + H_2O_2 \rightarrow OH^- + \cdot OH. \quad (16)$$

It should be noted that the reaction of electrons in water may be different from that in moist air. In moist air, electrons have a very high kinetic energy and can react with water vapor to generate reactive species. By contrast, in water, some electrons can become solvated electrons, which then participate in chemical reactions as a strong reductant [45].

2.2.2. OH reactions. ·OH is the key oxidant in AOPs. It can react with most organic and several inorganic compounds. The reactions of ·OH with various compounds mainly involve three different mechanisms [46, 47].

2.2.2.1. Abstraction of hydrogen atoms. The abstraction of hydrogen atoms mainly occurs when ·OH reacts with saturated aliphatic hydrocarbons or alcohols (see reaction (17)). This reaction yields H_2O and an organic radical (·M), and then ·M reacts with dissolved oxygen to generate the peroxy radical ·MOO (see reaction (18)); the peroxy radical is a strong oxidative species, and it can react with organic compounds via the hydrogen abstraction process (see reaction (19)) [46, 48]

$$\cdot OH + M - H \rightarrow \cdot M + H_2O, \quad (17)$$

$$\cdot M + O_2 \rightarrow \cdot MOO, \quad (18)$$

$$\cdot MOO + M'H \rightarrow MOOH + \cdot M'. \quad (19)$$

2.2.2.2. Electrophilic addition to double (triplet) bonds. The reactions of ·OH with unsaturated hydrocarbons are mainly attributed to this mechanism, by which ·OH can attack the C=C positions of unsaturated hydrocarbons, and then a C-centered radical (·M_2 (OH)C–CM_2) can be produced via the following reaction [46].

$$\cdot OH + M_2C = CM_2 \rightarrow \cdot M_2(OH)C\text{–}CM_2. \quad (20)$$

2.2.2.3. Electron migration. Electron migration mainly occurs when ·OH reacts with halogen-substituted compounds (see reaction (21)); in this case, the other two ·OH reaction mechanisms might not be favored.

$$\cdot OH + MX \rightarrow \cdot XM^+ + OH^-. \quad (21)$$

Due to these different reaction mechanisms, the speeds of the chemical reactions of ·OH with other contaminants are quite different. The second-order reaction rate constants of ·OH reacting with some selected substances are listed in table 1 [49–51]. Reaction rate constants can be used to determine the principal reaction when many compounds are present in one system, then the ·OH capture agent can be selected appropriately. For example, salicylic acid is usually selected as ·OH scavenger.

Table 1. The second-order reaction rate constants of ·OH with some selected substances.

Compounds	Rate constants (10^7 l mol^{-1} s^{-1})
Fe^{2+}	43
Cl^-	430
Br^-	1100
ClO_4^-	880
SO_4^{2-}	0.16
CO_3^{2-}	39
OH^-	1200
H_2O_2	2.7
Phenol	660
2-chlorophenol	1200
3-chlorophenol	720
4-chlorophenol	930
Bisphenol A	1000
1,1,2-trichloroethane	13
Acetic acid	1.6
Oxalic acid	0.14
4-nitrophenol	380
Pentachlorophenol	400
Salicylic acid	2200
t-butanol	420
Chlorobenzene	550
Xylene	670–750

2.2.3. O_3 reactions. In the electrical discharge plasma process, ·O is easily generated after the excitation and dissociation of oxygen molecules via high energy electron attack, and O_3 would be generated by the reaction of ·O radical with O_2, as shown in reaction (22).

$$\cdot O + O_2 + M \rightarrow O_3 + M. \quad (22)$$

O_3 can react with various compounds via two different reaction processes: direct O_3 oxidation and indirect O_3 oxidation (O_3 decomposition). The detailed reaction processes are discussed in the following sections.

2.2.3.1. Direct O_3 oxidation. O_3 molecules are characterized by dipolarity, nucleophilicity and eletrophilicity, and these properties contribute to three different reaction mechanisms for direct O_3 oxidation, which are Kerry's reaction, the electrophilic reaction, and the nucleophilic reaction [52–54]. Kerry's reaction is presented in equation (23), in which O_3 is added to C=C double bonds due to its dipolarity and generates carbonyl compounds and H_2O_2. The electrophilic reaction mainly occurs at positions with a high electron-cloud density in aromatic compounds. Usually, the *ortho-* and *para-* positions of the electron-donating groups have a high electron-cloud density, allowing electrophilic reactions to occur rapidly; whereas the *ortho-* and *para-* positions of the

electron-withdrawing groups have a quite low electron-cloud density, in which case electrophilic reactions would mainly occur at the *meta-* position. Therefore, O_3 can easily react with aromatic compounds those have electron-donating groups (such as phenols and aniline) via electrophilic reactions, from which some *ortho-* and *para-* substitution byproducts would be generated, as shown in equations (24) and (25). The nucleophilic reaction is similar to the electrophilic reactions, in which an oxygen atom with negative charge attacks a carbon atom with electron-withdrawing groups.

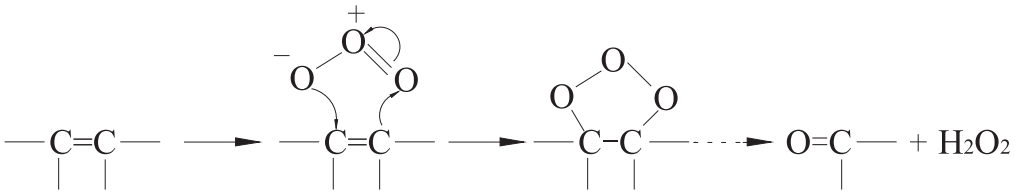

(23)

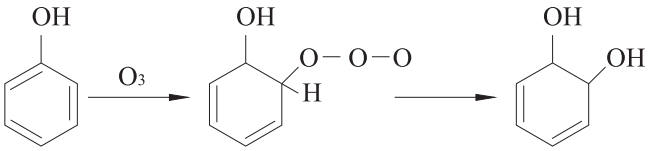

(24)

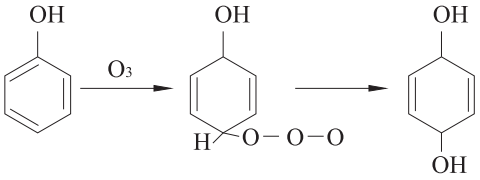

(25)

2.2.3.2. Indirect O_3 oxidation. The pathways of indirect O_3 oxidation are radical reactions. O_3 can undergo decomposition in basic solutions to generate ·OH and other reactive species, which have high oxidation potentials and thus can react with various compounds. The detailed reactions are as follows [55–57]:

$$O_3 + OH^- \rightarrow HO_2^- + \cdot O, \quad (26)$$

$$H^+ + HO_2^- \rightarrow H_2O_2, \quad (27)$$

$$H_2O_2 + O_3 \rightarrow HO_2^- + O_2 + \cdot OH, \quad (28)$$

$$O_3 + H_2O^- \rightarrow O_2 + \cdot O_2^- + \cdot OH, \quad (29)$$

$$H^+ + \cdot O_2^- \rightarrow HO_2 \cdot, \quad (30)$$

$$\cdot O_2^- + O_3 \rightarrow O_2 + \cdot O_3^-, \quad (31)$$

$$H_2O + \cdot O_3^- \rightarrow \cdot OH + OH^- + O_2, \quad (32)$$

$$\cdot H + O_3 \rightarrow \cdot HO_3, \quad (33)$$

$$\cdot O_3^- + H^+ \rightarrow \cdot HO_3, \quad (34)$$

$$\cdot HO_3 \rightarrow \cdot OH + O_2. \quad (35)$$

O_3 can also undergo catalytic decomposition by UV radiation and pyrolysis to generate atomic oxygen radicals, and then ·OH can be produced, as shown in equations (36)–(38) [58–60].

$$O_3 \xrightarrow{h\nu} \cdot O + O_2, \quad (36)$$

$$O_3 \xrightarrow{\text{pyrolysis}} \cdot O + O_2, \quad (37)$$

$$\cdot O + H_2O \rightarrow \cdot OH. \quad (38)$$

In addition, some carbon materials can also catalytically decompose O_3 to form other reactive species, such as ·OH (reactions (39)–(42)), which can enhance pollutant degradation efficiency [5]. Our previous research revealed that O_3 yield decreased in the presence of charcoal in a pulsed discharge plasma system, whereas the decoloration efficiency of dye-containing wastewater was enhanced [5].

$$O_3 + \text{H–carbon–H} \rightarrow \text{carbon–O} \cdot + H_2O_2, \quad (39)$$

$$O_3 + \text{carbon–OH} \rightarrow \text{carbon–O}_3 \cdot + \cdot OH, \quad (40)$$

$$\text{carbon–O}_3 \cdot \rightarrow O_2 + \text{carbon–O} \cdot, \quad (41)$$

$$O_3 + \text{carbon–O} \cdot \rightarrow \cdot O_2 + \text{carbon} + O_2. \quad (42)$$

In summary, direct O_3 oxidation and indirect O_3 oxidation occur simultaneously in the aqueous discharge plasma process, and their roles are dependent on solution pH to a certain extent. The speciation of organic contaminants is influenced by the solution pH. Organic contaminants are primarily in the molecular state when the solution pH value is lower than the contaminant pK_a, and primarily in the ionic form when the pH is higher than the pK_a. The reaction rate constants of O_3 with the ionic forms of organic compounds are much higher than those of O_3 with the molecular forms. For example, the reaction rate constants of O_3 with ionic *p*-nitrophenol and molecular *p*-nitrophenol are approximately $1.5 \times 10^7\,\text{l mol}^{-1}\,\text{s}^{-1}$ and $50\,\text{l mol}^{-1}\,\text{s}^{-1}$, respectively. Similarly, the reaction rate constant of O_3 with dissociated pentachlorophenol is approximately $3.1 \times 10^7\,\text{l mol}^{-1}\,\text{s}^{-1}$, while that of O_3 with the pentachlorophenol molecule is $6.7 \times 10^4\,\text{l mol}^{-1}\,\text{s}^{-1}$ [61].

2.2.4. H_2O_2 reactions. H_2O_2 can directly or indirectly participate in the contaminant removal process. The oxidation potential of H_2O_2 is not very high, and thus the contribution of direct H_2O_2 oxidation to the degradation of contaminants is often quite weak. Usually, H_2O_2 can be decomposed into ·OH in electrical discharge plasma process via several pathways, such as electron collisions (equation (16)), reaction with O_3 (equation (24)), and UV photolysis (equation (43)) [4, 61].

$$H_2O_2 + h\nu \rightarrow \cdot OH + \cdot OH. \quad (43)$$

To enhance the pollutant degradation efficiency, several metallic cations are usually selected to catalytically decompose H_2O_2 to generate ·OH in electrical discharge plasma (see reactions (44)–(48)) [62, 63]. Furthermore, nano-TiO_2 is another common catalyst widely used in electrical discharge plasma process because it can be activated by the discharge plasma to generate holes and electrons, which then reacts with H_2O_2 to produce oxidative species, as shown in equations (49)–(51) [64, 65].

$$H_2O_2 + Fe^{2+} \rightarrow \cdot OH + Fe^{3+} + OH^-, \quad (44)$$

$$\cdot OH + Fe^{2+} \rightarrow OH^- + Fe^{3+}, \quad (45)$$

$$H_2O_2 + \cdot OH \rightarrow HO_2 \cdot + H_2O, \quad (46)$$

$$H_2O_2 + Cu^{2+} \rightarrow H^+ + (Cu^{2+}OOH^-)^+, \quad (47)$$

$$(Cu^{2+}OOH^-)^+ \rightarrow 1/2O_2 + \cdot OH + Cu^+, \quad (48)$$

$$TiO_2 + h\nu \rightarrow e^-_{cb} + h^+_{vb}, \quad (49)$$

$$e^-_{cb} + H_2O_2 \rightarrow OH^- + \cdot OH, \quad (50)$$

$$h^+_{vb} + H_2O_2 \rightarrow H^+ + HO_2 \cdot . \quad (51)$$

In our research, Cu^{2+} and Fe^{2+} were selected to improve polyvinyl alcohol (PVA) degradation in a hybrid gas–liquid pulsed discharge plasma system, and we observed that the presence of both Cu^{2+} and Fe^{2+} significantly enhanced PVA degradation during the pulsed discharge plasma process, whereas the detected H_2O_2 concentration was much lower in the presence of Cu^{2+} or Fe^{2+} [66]; these phenomena suggested that some amounts of H_2O_2 were catalytically decomposed by Cu^{2+} and Fe^{2+} in electrical discharge plasma.

In addition, some carbon materials can catalytically decompose H_2O_2 to form ·OH and HO_2· (reactions (52) and (53)), which then enhance the pollutant degradation efficiency [60, 67]. Our previous research illustrated that the H_2O_2 yield decreased in the presence of charcoal in a pulsed discharge plasma system, whereas the decoloration efficiency of dye-containing wastewater was enhanced [5]

$$\text{carbon} + H_2O_2 \rightarrow \text{carbon}^+ + \cdot OH + OH^-, \quad (52)$$

$$\text{carbon}^+ + H_2O_2 \rightarrow \text{carbon} + HO_2 \cdot + H^+. \quad (53)$$

2.2.5. Reactions of other active radicals. Some short-lived species (·H, ·NO and ·O, etc) are produced in the discharge plasma process, and these reactive species also play quite significant roles in wastewater treatment.

·H is a reductant, and it can react with some metal ions via reduction–oxidation reactions. This mechanism is usually utilized in the removal of heavy metals via the glow discharge plasma process. For example, Cr(VI) can be reduced rapidly by ·H to produce Cr(V) and Cr(III), according to reactions (54) and (55) [68, 69]. Therefore, ·H can be used to transform highly charged metal ions into low-charged metal ions, and thus decrease the toxicity of some metal ions.

$$\cdot H + Cr(VI) \rightarrow H^+ + Cr(V), \quad (54)$$

$$\cdot H + Cr(VI) \rightarrow H^+ + Cr(III). \quad (55)$$

·NO is mainly generated in the arc discharge plasma process, and its role is mainly to acidify solutions via the generation of N-containing acids such as NO_3^- and NO_2^-. The detailed reactions are presented in equations (56)–(60):

$$N_2 + 2e \rightarrow 2 \cdot N, \quad (56)$$

$$\cdot N + \cdot O \rightarrow NO_2, \quad (57)$$

$$\cdot N + O_2 \rightarrow NO + \cdot O, \quad (58)$$

$$\cdot OH + NO_2 \rightarrow HNO_3, \quad (59)$$

$$\cdot OH + NO \rightarrow HNO_2. \quad (60)$$

·O is a quite strong oxidant, and it plays very significant roles in the degradation of contaminants. ·O can react with O_2 and H_2O molecules to produce O_3 and ·OH (see equations (22) and (38)), and it can also react with hydrocarbons, as shown in equations (61)–(63) [70]:

$$C_2H_3 + 4 \cdot O \rightarrow 2CO_2 + 3 \cdot H, \quad (61)$$

$$C_2H_2 + 5 \cdot O \rightarrow 2CO_2 + H_2O, \quad (62)$$

$$C_2H_2O + 4 \cdot O \rightarrow 2CO_2 + H_2O. \quad (63)$$

In addition, active ions are quite important components formed in the electrical discharge plasma process. However, many research studies have been conducted to investigate the roles of active radicals and molecules during wastewater treatment by electrical discharge plasma; little attention has been paid to the active ions. In fact, some active ions, such as N^+, N_2^+, $\cdot O_2^-$, $O^-\cdot$, H_2O^+, O_3^-, and $\cdot O_2^-$, can also be generated and play certain roles in contaminant degradation.

Some N-containing ions, such as N^+ and N_2^+, can be generated when N_2 molecules are dissociated by electron attack in electrical discharge plasma process, and the possible reactions are shown in the following equations (64)–(68) [71, 72]. N^+ and N_2^+ can contribute to the formation of more ·OH. Zhang *et al* [72] discussed the roles of N-containing ions such as N^+ and N_2^+ in chlorophenol removal from wastewater in a pulsed discharge plasma system.

$$N_2 + e \rightarrow N + N^+ + 2e, \quad (64)$$

$$N_2 + e \rightarrow N_2^+ + 2e, \quad (65)$$

$$N_2^+ + H_2O \rightarrow N_2^+(H_2O), \quad (66)$$

$$N_2^+ + H_2O \rightarrow \cdot NH + \cdot OH, \quad (67)$$

$$N_2^+(H_2O) + H_2O \rightarrow H_3O^+ + N_2 + \cdot OH. \quad (68)$$

In the presence of nano-TiO_2, electrical discharge plasma can excite the nano-TiO_2 to generate electrons (e^-) and holes ($h+$ vb). It has been suggested that the electrons can attack oxygen molecules to form single atomic oxygen radical anions ($\cdot O^-$) and superoxide radical anions ($\cdot O_2^-$); subsequently, $\cdot O_2^-$ and $\cdot O^-$ can be transformed into $\cdot O_2$ radical and $\cdot O$ via reactions with $h+$ vb on the surface of the nano-TiO_2, leading to increased O_3 generation via the following possible reactions (reactions (69)–(73)) [73–75]. In an appropriate alkali environment, $HO_2\cdot$ can also be converted to $\cdot O_2^-$ (reaction (30)), and the presence of $\cdot O_2^-$ in the solution is essential for bacterial inactivation by the plasma [76].

$\cdot O_2^-$ have a relatively long lifetime in solution (5 s at 1.0×10^{-6} M), which is much higher than that of $\cdot OH$ (200 μs at 1.0×10^{-6} M) [77, 78]. Perni *et al* [79] reported that plasma-generated O atoms and $\cdot O_2^-$ played the dominant roles in *Escherichia coli* inactivation. In addition, it must be noted that if the solution pH value is sufficiently low, $\cdot O_2^-$ will be converted to $HO_2\cdot$, which can also participate in bacteria inactivation via penetrating the cell membrane and damaging intercellular components [80].

$$O_2 + e^- \rightarrow 2 \cdot O^-, \quad (69)$$

$$O_2 + e^- \rightarrow \cdot O_2^-, \quad (70)$$

$$\cdot O_2^- + h_{vb}^+ \rightarrow \cdot O_2, \quad (71)$$

$$\cdot O^- + h_{vb}^+ \rightarrow \cdot O, \quad (72)$$

$$\cdot O + O_2 \rightarrow O_3. \quad (73)$$

In the glow discharge plasma process, the positive gaseous ion H_2O^+ can react with H_2O to produce $\cdot OH$ after it diffuses into the liquid phase via the driving force of ion wind (see equation (10)) [81]. The energy of H_2O^+ is very high, and thus the $\cdot OH$ yield is high, and then large amounts of H_2O_2 can be formed via $\cdot OH$ recombination. It has been suggested that the yield of H_2O_2 per mole of electrons in glow discharge plasma can surpass the yield limit of Faraday's law [81].

Negative ions such as O_3^- and O_2^- are formed in corona discharge in oxygen above the water surface, and these species can lead to the formation of O, O_3, and $\cdot OH$ (see reactions (74)–(77) and (38)) [82, 83]. In addition, the combination of ions and neutral species generated in gas phase discharge plasma is reported to be responsible for solution pH changes [83].

$$e + O_2 \rightarrow O + O^-, \quad (74)$$

$$O^- + O_2 \rightarrow O + O_2^-, \quad (75)$$

$$O^- + 2O_2 \rightarrow O_2 + O_3^-, \quad (76)$$

$$O_3^- + O_2 \rightarrow O_2 + O_3 + e. \quad (77)$$

In summary, the chemical effects of discharge plasma are quite complex, including radicals, ions, and molecular reactions; many parameters can affect these reactions. For instance, a high solution conductivity can lead to relatively lower formation rates of reactive species [84, 85]. Some species may be able to enter the liquid phase from the discharge electrodes and thus influence the chemical properties of solutions. The material quality of the discharge electrodes can also affect the chemical reactions [86]. Moreover, the type of carrier gas between the electrodes, such as O_2, N_2, or air, can significantly influence the variety and yield of oxidative species [71, 87, 88]. It is important to note that post-discharge reactions deriving from long-lived reactive species can also occur in the discharge plasma process, which can further enhance the removal efficiency of contaminants [89].

3. Reactive species measurement

Various reactive species, including $\cdot OH$, $\cdot O$, H_2O_2 and O_3, can be generated in electrical discharge plasma process. It is of great significance to measure these reactive species quantitatively or qualitatively to explore the discharge plasma process and mechanisms, and to provide guidance for utilizing electrical discharge plasma for contaminant removal. Recently, several methods have been proposed to measure these reactive species. An introduction to these methods is reviewed below.

3.1. H_2O_2 measurement

H_2O_2 is a relatively long-lived species, and it is usually detected directly using traditional chemical methods, such as iodometry method [43, 90], potassium titanium colorimetric method [91, 92], and direct instrumental analysis [93]. The potassium titanium colorimetric method has received great attention. Wang *et al* [92] employed the potassium titanium colorimetric method to measure H_2O_2 concentration during the gas–liquid pulsed discharge plasma process. They also evaluated the effects of radical scavengers on H_2O_2 formation. They observed that the presence of *n*-butanol significantly inhibited H_2O_2 formation, whereas adding Na_2CO_3 increased the H_2O_2 concentration. It is known that *n*-butanol and Na_2CO_3 are both $\cdot OH$ scavengers, and the $\cdot OH$ can recombine to form H_2O_2. Therefore, Wang *et al* [92] deduced that $\cdot OH$ recombination is one mechanism for H_2O_2 formation, and that other reactions also participate in its formation. Under alkaline conditions (Na_2CO_3 addition), dissolved oxygen can undergo electrolytic dissociation on the surface of electrodes, which would contribute to the formation of some additional amounts of H_2O_2.

The H_2O_2 yield is affected by the carrier gas in the discharge plasma process. We evaluated the H_2O_2 formation in a

hybrid gas–liquid pulsed discharge plasma system with various carrier gases, and the highest H_2O_2 yield was observed for bubbling O_2, followed in descend for bubbling air, while the lowest H_2O_2 yield was observed for bubbling N_2 [94]. When N_2 is selected as the carrier gas, ·OH is generated via the reactions of N-containing species with water molecules (see reactions (60) and (61)), which then recombine to form H_2O_2; however, O-containing species react with water molecules directly to form H_2O_2 when O_2 is selected as the carrier gas, in addition to generating ·OH. Therefore, a relatively high H_2O_2 yield is obtained when bubbling O_2 compared with that obtained when bubbling N_2.

The H_2O_2 yield is also affected by the solution pH and conductivity. Hsieh reported that the greatest H_2O_2 concentration was observed in solution pH = 4 and decreased as the pH value increased in alkaline conditions; an increase in solution conductivity also led to a decrease in H_2O_2 concentration in a gas–liquid film plasma system [95]. Increasing the solution pH or the amount of solute introduces more ions, which can influence discharge plasma occurrence due to the changes in solution conductivity [96]. A higher solution conductivity can lead to a lower H_2O_2 yield due to UV and thermal effects; this is because a larger discharge current, shorter discharge streamer length, higher power density, higher plasma temperature and UV radiation occur [26].

3.2. O_3 measurement

O_3 is a relatively long-lived species, and it can be easily detected quantitatively. The iodometry method and indigo method are two of the main techniques used to measure both gaseous and dissolved O_3 concentrations [97, 98]. Some oxidative species, including NO_x, H_2O_2 and ·O, can oxidize iodide and indigo as well, and therefore there exist some errors in O_3 concentration measurement; however, it is very difficult to distinguish the contributions of various active species to 'O_3 concentration'. As a result, the concept of 'O_3 equivalent concentration' has been proposed to characterize the oxidation potential of a discharge plasma system, which is calculated as the 'O_3 concentration' [99, 100]. In addition, the gaseous O_3 concentration can also be measured directly by an O_3 monitor [101]. Although the chemical methods reviewed above can measure the O_3 concentration quantitatively, they are unable to analyze the O_3 production process, O_3 spatial distribution, and O_3 dynamics.

Recently, laser absorption methods have been proposed to analyze O_3 generation behaviors in gaseous discharge plasma process [102–104]. Ono and Oda [102] investigated O_3 generation and distribution in discharge plasma via a two-dimensional laser absorption method, they found that the O_3 density increased continually when the post-discharge time was lower than 100 μs and then gradually migrated to the ground electrode when the post-discharge time was higher than 1 ms. The effect of humid air on O_3 distribution was also evaluated in the pulsed corona discharge plasma process, and the O_3 yield and formation time decreased when water vapor was added to the system [103].

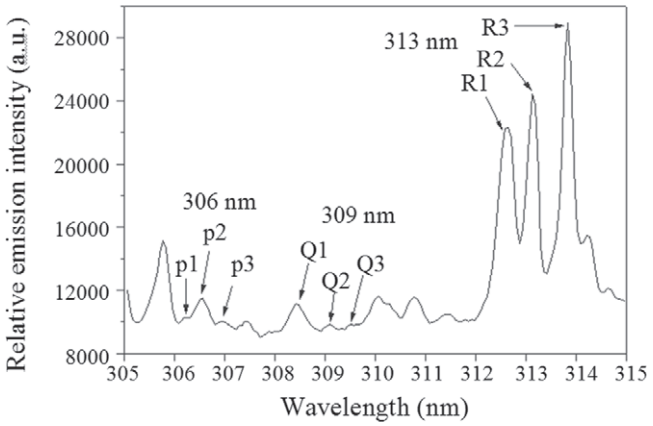

Figure 1. Typical optical emission spectrum obtained in a multi-point-to-plate pulsed discharge plasma system.

In addition, the O_3 yield in aqueous solution is affected by the aqueous surface tension in discharge plasma process [105]. Our research found that the addition of small amounts of nonoic acid (NA), lactic acid (LA), and acetic acid (AA) to solutions decreased the aqueous surface tension in a surface discharge plasma system, as a result of which the O_3 equivalent concentration in solution was enhanced [105].

3.3. •OH measurement

As a quite short-lived species, ·OH is more difficult to detect than O_3 and H_2O_2. Usually, it is measured using indirect methods such as radical scavengers [92, 106–108], paramagnetic resonance [109], spin trapping [110], chromatography [111], and absorption [112]; among these, the radical scavenger method is widely employed, in while salicylic acid, 4-hydroxybenzoate, *n*-butanol, Na_2CO_3, isopropanol, and dimethylsulfoxide are generally selected as ·OH scavengers. Bian *et al* [107] investigated the ·OH generation rate using 4-hydroxybenzoate as the ·OH scavenger during the pulsed discharge plasma process. They found that the ·OH formation rate was approximately 3.49×10^{-7}, 3.56×10^{-7}, 3.21×10^{-7} and 1.94×10^{-7} mol l^{-1} s^{-1} when N_2, argon (Ar), air, and O_2 was selected as the carrier gas, respectively. Wang *et al* [92] selected *n*-butanol and Na_2CO_3 to scavenge ·OH and found that the relative concentration of ·OH decreased after *n*-butanol and Na_2CO_3 addition. Fluorescence spectroscopy is another frequently-used method for ·OH measurement, and terephthalic acid is usually selected to scavenge ·OH in this case because terephthalic acid can react with ·OH to produce hydroxyterephthalic acid. The latter can be analyzed via fluorescence spectroscopy, and then the ·OH concentration can be calculated based on the spectral intensity of hydroxyterephthalic acid [111].

The above methods for ·OH measurement are mainly based on chemical probes, some of which cannot quantitatively measure the ·OH concentration. More importantly, such methods are unable to analyze the ·OH generation process, spatial distribution, and dynamics. Recently, optical emission spectroscopy (OES) has received great attention in detecting ·OH in the discharge plasma process because it can detect

·OH *in situ*. In such case, the ·OH generation process and spatial distribution can also be obtained [44, 86, 113–115]. The main principle for ·OH detection by OES is that some amounts of ·OH are in an excited state (upper state) due to the attack of high-energy electrons; these excited ·OH would transit spontaneously from the upper state to the lower state, accompanied by the liberation of photons of different wavelengths. Specific photons are captured by the detector, and their intensity is proportional to the ·OH concentration. A typical optical emission spectrum from the pulsed streamer discharge plasma process was obtained in our research, as shown in figure 1. Sun *et al* [113] studied gaseous ·OH formation and distribution in a negative pulsed discharge plasma system via OE, and reported that a higher pulse repetition rate, lower air flow rate, and smaller nozzle electrode diameter were all beneficial to obtain relatively higher ·OH concentrations; ·OH mainly appeared around the high voltage electrode. Liu *et al* [114] reported that increasing the He and Ar content in mixed N_2 + He and N_2 + Ar gases increased the intensity of ·OH in a pulse discharge plasma system via OES analysis, whereas increasing O_2 contents in O_2 + N_2 mixture gases decrease ·OH yield. In addition to ·OH detection in gas phase, OES could also analyze ·OH in aqueous solutions. Sun *et al* [87] studied the influences of discharge pattern, discharge polarity, and O_2 flow rate on ·OH generation in solution by OES, and found that the highest ·OH yield was observed in spark discharge; positive discharge was more beneficial for ·OH formation than negative discharge; increasing O_2 flow rate benefited ·OH generation to a certain extent. Our previous research evaluated ·OH generation via OES analysis in a gas–liquid pulsed discharge plasma combined with nano-TiO_2 system, and found that appropriate levels of nano-TiO_2 addition could increase the relative intensity of ·OH [44]. In addition, the highest ·OH concentration was observed in Ar atmosphere, followed by air atmosphere, and the lowest was observed in oxygen [116, 117]. It is known that N_2^+ can be generated in the discharge plasma process, which can result in the generation of ·OH via reaction with H_2O (see equation (67)). Ar can also be excited by high-energy electrons to form Ar^+, which then reacts with H_2O molecules to form ·OH radicals (equations (78) and (79)) [116, 118].

$$Ar \xrightarrow{e} Ar^+ + e, \tag{78}$$

$$Ar^+(H_2O) + H_2O \rightarrow H_3O^+ + Ar + \cdot OH. \tag{79}$$

Although OES diagnosis can be used to analyze the ·OH formation process and spatial distribution, it is unable to actually calculate the absolute ·OH concentration. Furthermore, it can only passively capture photons released from the ·OH spontaneous transition, and therefore, the measurement accuracy and temporal-spatial resolution are both low.

Another method for ·OH radical diagnosis is laser-induced fluorescence (LIF) [119–121]. A significant number of ·OH generated in the discharge plasma are in a relatively lower state. These can be excited by laser to transit to the upper state; and then photons can be liberated when the excited ·OH migrate to the lower state. These photons are captured and their intensity is proportional to the ·OH concentration. Therefore, compared with OES, LIF is an active method for ·OH detection, and its measurement accuracy and temporal-spatial resolution are both higher. More importantly, the two-dimensional distribution and density of ·OH can be obtained by LIF analysis combined with an ICCD camera. Ono and Oda [119] reported that ·OH was mainly produced in the discharge plasma area, and the highest ·OH density was observed at a post-discharge time of 40 μs. They also reported that the absolute density of ·OH in humid air with 3% H_2O at 50 μs post-discharge time was approximately 1×10^{15} cm^{-3}. ·OH formation and dynamics on the water surface were also evaluated in the discharge plasma process [111, 122–124]. Kanazawa *et al* [111] studied ·OH formation on the liquid surface in the pulsed discharge plasma process by LIF and found that some gaseous ·OH could migrate and dissolve into the water.

Although LIF can provide a high measurement accuracy, high temporal-spatial resolution, and quantitative determination for ·OH diagnosis, at present, it can only detect ·OH in the gas phase.

3.4. Other reactive species measurements

In addition to H_2O_2, O_3, and ·OH, the identification and quantification of other reactive species such as ·H, $\cdot O_2^-$, aqueous electron, N^*, ·O, and singlet oxygen ($^1O_2$) have also received great attention due to their significant roles in the discharge plasma process. Chemical probes and spectrum diagnosis are two main methods for their measurement.

·H is generated when water molecules are dissociated by electron attack (equation (4)), and then $HO_2\cdot$ is formed via the reaction of ·H with O_2; while $\cdot O_2^-$ and $HO_2\cdot$ speciation is a function of solution pH (see equations (80) and (81)) [125]. $\cdot O_2^-$ has a relatively high oxidation potential and can participate in the decomposition of contaminants, and it can also affect the formation of other species (see equations (30), (82) and (83)). Sahni and Locke [126] quantitatively calculated the concentrations of $\cdot O_2^-$ and ·H by tetranitromethane and nitroblue tetrazolium chloride scavenging probes. ·H radicals can also be detected by OES analysis. Sato *et al* [127] detected ·H radicals in solution during the pulsed discharge plasma process by OES and found that increasing the solution conductivity was not beneficial for ·H radical formation.

$$\cdot H + O_2 \rightarrow HO_2\cdot, \tag{80}$$

$$HO_2\cdot \xleftrightarrow{pKa=4.8} \cdot O_2^- + H^+, \tag{81}$$

$$HO_2\cdot + \cdot O_2^- + H^+ \rightarrow H_2O_2 + O_2, \tag{82}$$

$$HO_2\cdot + e^- + H^+ \rightarrow H_2O_2. \tag{83}$$

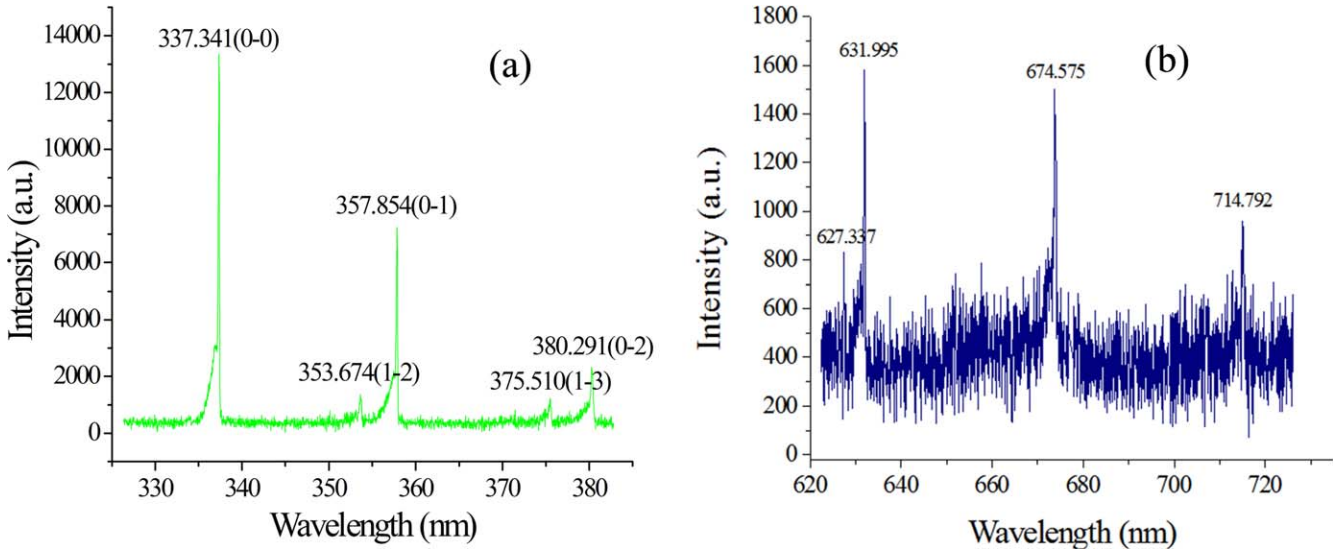

Figure 2. Typical optical emission spectrum obtained in a dielectric barrier discharge plasma system ((a) N_2 atmosphere; (b) O_2 atmosphere).

The aqueous electron is a strong reductant in the electrical discharge plasma process, and it can be generated via subexcitation electrons (energy <7.4 eV) captured by surrounding water molecules, as shown in reaction (84) [128]. The presence of a reductant might benefit the removal of some contaminants by reduction mechanisms. Joshi *et al* [43] reported that the initiation rate constant of aqueous electron formation was independent of time and that its yield increased with increasing applied discharge voltage. The aqueous electron plays significant roles in the discharge plasma process. Phosphate could rapidly react with the aqueous electron with a reaction rate constant of more than $10^7\ M^{-1}\ s^{-1}$, and it is usually selected as the aqueous electron scavenger [129–131]. Leitner observed that there was an obvious decrease in atrazine degradation efficiency in an electrohydraulic discharge plasma system when small amounts of $H_2PO_4^-$ were added [129]. Zhang *et al* [130] reported that the microcystin-LR degradation efficiency decreased in the presence of $H_2PO_4^-$ in a glow discharge plasma system. In our research, to evaluate the role of $\cdot O_2^-$ and the aqueous electron in *p*-nitrophenol degradation in a pulsed discharge plasma system, 1,4-benzoquinone and $H_2PO_4^-$ were also selected to capture $\cdot O_2^-$ and aqueous electrons, respectively; we found that the *p*-nitrophenol degradation efficiency significantly decreased after adding small amounts of 1,4-benzoquinone and $H_2PO_4^-$ [131].

$$H_2O + e^- \rightarrow e_{aq}^-. \quad (84)$$

The typical optical emission spectrum obtained in a dielectric barrier discharge plasma system under N_2 atmosphere and O_2 atmosphere is shown in figure 2, where N-containing species (figure 2(a)) and O-containing species (figure 2(b)) can be observed. Singlet oxygen is unstably excited oxygen, and it is characterized as strong oxidation potential and short life [132]. Singlet oxygen can be detected via chemical probe or spectroscopic diagnosis. NaN_3 is an effective quencher of singlet oxygen, and the addition of NaN_3 to wastewater containing phenol can cause an approximately 40% decrease in phenol degradation efficiency [133]. Ono and Oda measured the excited oxygen in a pulsed discharge plasma system by LIF and reported that the excited oxygen was mainly generated in the secondary streamer channels, and its density could reach approximately $10^{14}\ cm^{-3}$ around the high voltage electrode [134]. The addition of water vapor in the discharge plasma process could enhance the excited oxygen content [135]. Hong *et al* [136] observed excited oxygen using OES in an argon–oxygen plasma jet system.

4. Mass transfer of reactive species

Chemical reactions usually occur in the bulk gas phase, liquid phase, and at the gas–liquid interface due to transport processes in discharge plasma systems. Reactive species can be formed and react with each other among these different phases. Taking H_2O_2 formation as an example, ·OH recombination can occur in the gas, in the liquid, or at the interface to form H_2O_2, as shown in reactions (85)–(87). Therefore, chemical reactions are important factors affecting mass transfer in interphase. If a gaseous species is absorbed into the liquid phase with no reactions, its mass transfer from the gas phase to the liquid will be slow; however, if a compound in the liquid can react with this gaseous species as soon as it enters the liquid phase, its mass transfer from the gas phase to the liquid will be much higher [24].

$$2\ \cdot OH_{(g)} + M \rightarrow H_2O_{2(g)} + M, \quad (85)$$

$$2\ \cdot OH_{(aq)} \rightarrow H_2O_{2(aq)}, \quad (86)$$

$$2\ \cdot OH_{(int)} \rightarrow H_2O_{2(int)}. \quad (87)$$

Mass transfer processes in discharge plasma usually involve neutral species, ions, and electrons. The processes of the interfacial reactions of neutral species include gas kinetic collisions, adsorption onto particle surfaces or into particles, desorption from particles, diffusion in the condensed phase, and chemical reactions onto particle surfaces. The Langmuir–Hinshelwood and Eley–Rideal processes are two common mechanisms for the mass transfer of neutral species [137].

The transport of ions across the gas–liquid interface includes positive ions and negative ions. Atomic-scale simulations were employed to evaluate the interaction of positive ions with the water surface [138]; in which the sputtering of water molecules from the interface and ion penetration depth were both involved. It is difficult for positive ions to penetrate into liquid. O^+ ions with an energy of 100 eV can only penetrate beyond the liquid surface for nearly 3 nm [138]. Negative ions transport across the gas–liquid interface is relatively unexplored because they do not have positive potential energies, and they are more energetically equivalent to neutral species. Cserfalvi and Mezei [139] developed a secondary electron emission mechanism to evaluate the influence of negative ions on the liquid surface.

The transport of electrons across the gas–liquid interface generally includes two types. The first one is highly energetic electrons, which can excite, dissociate or ionize water molecules; the other one is low-energy electrons, which usually become solvated electrons [45]. The highly energetic electrons often enter the water or cluster as an electron beam, which then initiates lots of chemical reactions to produce reactive species. The solvated electrons derived from the low-energy electrons can also participate in some chemical reactions, leading to the generation of some reactive species; however, these reactions are dependent on the solvated electron concentration, solution pH, and dissolved gases. For instance, the solvated electrons can combine with dissolved oxygen to form $\cdot O_2^-$ [140]. It must be noted that although the lifetime of the solvated electrons is as short as other short-lived radicals such as ·OH, they are an important precursor for plasma-induced chemical reactions at the gas–liquid interface.

The reactor configuration, experimental conditions, and external environment can all affect the reactive species mass transfer. Bian *et al* [107] reported that better performances for reactive species mass transfer and *p*-chlorophenol degradation were obtained when using metal mesh as the ground electrode than using stainless steel plate ground electrode. Pawlat *et al* [98] designed a dynamic foam reactor to improve the reactive species mass transfer, in which the wastewater was firstly foamed before entering into the discharge plasma region. It is worth noting that the appropriate gas flow rate could enhance the diffusion of gaseous reactive species into solution [141]. Tsouris *et al* [142, 143] employed micro-wall plates to reduce the bubble size, which strongly enhanced the O_3 mass transfer into liquid. Instead of a conventional bubble contactor, a microbubble generator was employed by Chu *et al* [144] during dyestuff wastewater treatment by ozonation, and they found that the microbubble generator clearly enhanced the diffusion of O_3 in solution due to the formation of large numbers of microbubbles with an average diameter lower than 60 μm.

The presence of organic acids can change the solution properties and thus affect the morphology and distribution of bubbles, which then further influence the diffusion of species [145]. Cheng [146] reported that appropriate amounts of heptanoic acid, nonyl acid, or *n*-heptyl alcohol in solution could improve the diffusion effect of O_3, and he attributed this phenomenon to the enhancement of the mass transfer coefficient and equilibrium concentration of O_3 in the liquid phase. In our research, we found that the presence of organic acids decreased the solution surface tension, which benefited the formation of small bubbles and their uniform distribution (see figure 3), and then the O_3 equivalent concentration increased, resulting in a relatively higher AO7 decoloration efficiency in the discharge plasma process.

The diffusion of oxidative species in the discharge plasma process is also affected by several operating conditions [66, 147]. A more severe disturbance was observed for the plasma–liquid reaction surface at a higher discharge voltage, which would improve the oxidative species mass transfer [66]. A decrease in the electrode distance could enhance the O_3 diffusion into the liquid phase in gas phase discharge plasma over the water surface [147]. Convection or fluid motion in the liquid phase is an important process to distribute reactivity at the plasma–liquid boundary. Bulk gas convection associated with plasma occurs when the discharge plasma is maintained in streamer discharge or corona (producing ionic wind) [148, 149]. Shimizu *et al* [150] reported that convection was induced in the liquid with speeds of several cm s^{-1}, sufficient to dominate over diffusion. Burlica *et al* [151] reported that the gas flow rate could significantly affect hydrogen peroxide mass transfer in liquid. The contact time for a fluid element in plasma zone will be decreased at a higher gas flow rate, which then benefits hydrogen peroxide accumulation.

The translation of wastewater into a liquid film or an aerosol is an efficient way to enhance the reactive species mass transfer, especially for atomization which greatly improves the collision chance between the reactive species and contaminant molecules. Li *et al* [29] developed a reactive species injection reactor for wastewater treatment, in which the gaseous reactive species was injected completely into the wastewater under the driving force of gas flow, which thus enhanced the reactive species utilization efficiency; the experimental results showed that more than 95% of decoloration efficiency for wastewater containing methyl red, reactive brilliant blue and cationic red was obtained within 4 min's discharge plasma treatment.

5. Reactive species generation and pollutant removal in different discharge plasmas

In the electrical discharge plasma process, the generation of reactive species plays significant roles in the degradation of organic pollutants, and the generation of these reactive species is dependent on the discharge plasma type, such as DBD

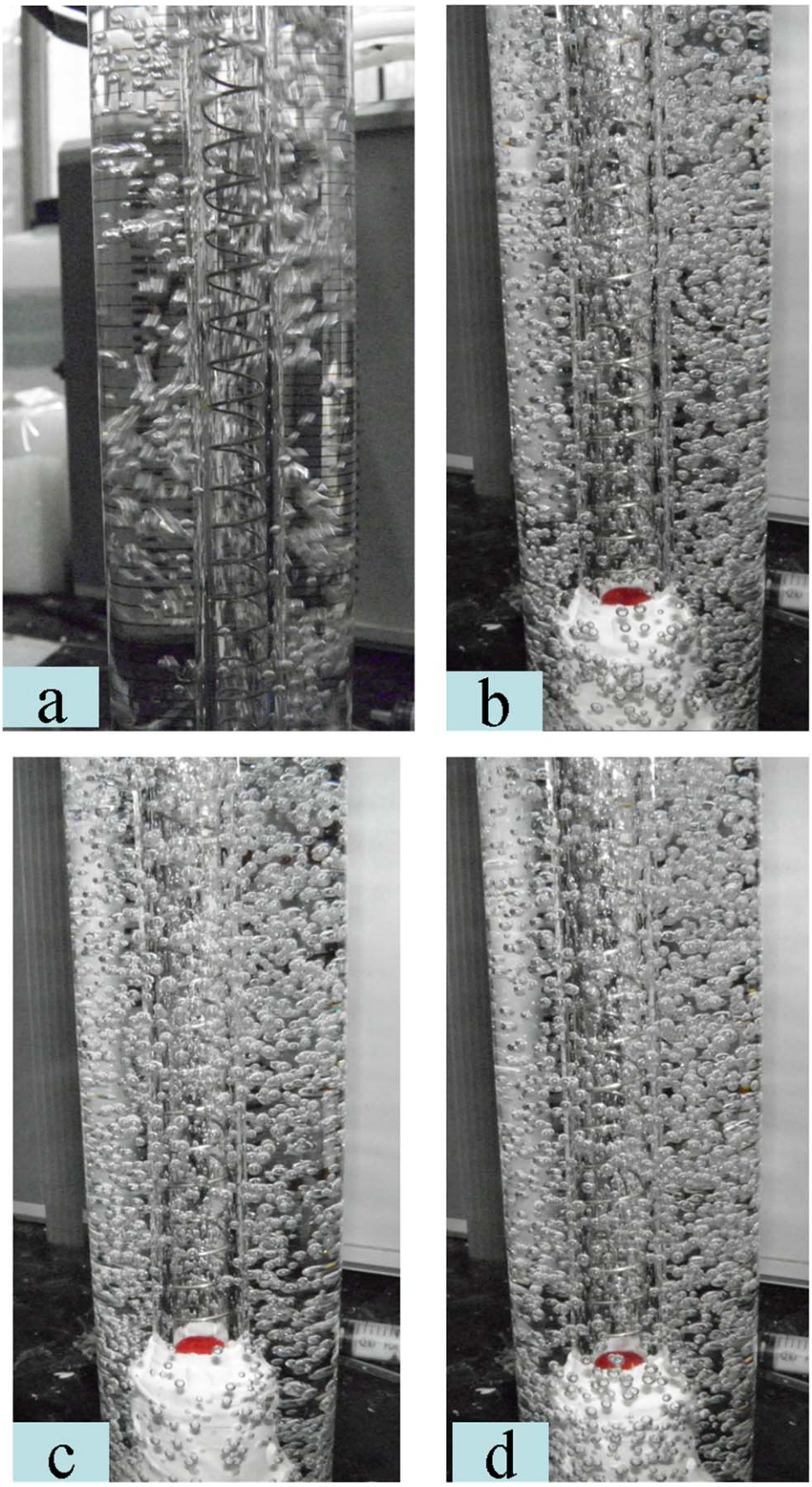

Figure 3. Photos of bubbles under different organic acid additions: (a) no additive; (b) acetic acid addition; (c) lactic acid addition; (d) nonoic acid addition.

Table 2. Reactive species generation and energy yield in different discharge plasmas.

Discharge plasmas	Conditions	$G_{\cdot OH}$ (mmol l^{-1} kWh^{-1})	$G_{H_2O_2}$ (mmol l^{-1} kWh^{-1})	G_{O_3} (mmol l^{-1} kWh^{-1})	References
Surface DBD	19.6 kV, 21.2 W	—	—	~15.1	[105]
Gas phase DBD	60 W	~3.56	~0.155	~0.212	[152]
Pulsed discharge in liquid	60 Hz, 66 W	—	~34.1	—	[153]
Pulsed discharge in liquid	100 Hz, 16 kV	—	~23.1	~1.08	[154]
Pulsed discharge in liquid	150 Hz, 20 kV	~19.26	~103.8	—	[105]
Pulsed discharge in liquid	140 Hz, 25 kV	~15.56	~224.2	~1.28	[155]
Pulsed discharge in liquid	64 W, 45 kV	~3.77	~34.3	—	[156]
Gliding arc discharge	320 W		~2.21	~0.016	[157]
Contact glow discharge	500 V, 100 mA	—	~411.8	—	[158]
DC diaphragm glow discharge	750 V, 140 mA	—	~96.0	—	[159]
AC diaphragm glow discharge	50 Hz, 77 W	—	~168.3	—	[160]

plasma, surface discharge plasma (a type of DBD plasma), pulsed discharge plasma, gliding arc discharge plasma, and glow discharge plasma. O_3, H_2O_2, and ·OH radicals are three main reactive species generated in discharge plasmas, and their measurement methods are relatively mature; and thus the generation and energy yield of these reactive species in different discharge plasmas are compared and listed in table 2. Here, the energy yield for reactive species generation (G) is calculated as the reactive species concentration divided by the energy consumption.

During wastewater treatment by traditional gas phase DBD plasma, O_3 is first generated in the gas phase and then diffuses into the liquid phase; for ·OH generation in the liquid phase, the attacks of high-energy electrons on water molecules in the gas–liquid interface play decisive roles, as well as the mutual reactions of ·O with water molecules (see reactions (8)–(10), and (38)); for H_2O_2 generation in the liquid phase, the recombination of ·OH plays a significant role; therefore, the energy yields for ·OH and H_2O_2 generation in the liquid phase are relatively low in traditional gas phase DBD plasma due to the limitation of mass transfer. Tang *et al* [152] selected gas phase DBD plasma to degrade 2,4-dinitrophenol in wastewater, and the energy yields for ·OH, H_2O_2, and O_3 generation were approximately 3.56 mmol l^{-1} kWh^{-1}, 0.155 mmol l^{-1} kWh^{-1}, and 0.212 mmol l^{-1} kWh^{-1}, respectively. In our previous research, a gas phase surface discharge plasma (one type of DBD) was developed to treat wastewater, and in this kind of reactor system, the reactive species were first generated in the gas phase and then injected into the liquid phase by high-speed gas flow, and thus, the mass transfer of the reactive species was enhanced; the energy yield for O_3 generation was approximately 15.1 mmol l^{-1} kWh^{-1}, which was much higher than that in traditional gas phase DBD plasma.

During wastewater treatment by liquid pulsed discharge plasma, high-energy electrons are generated directly in the liquid phase; collisions between the high-energy electrons and water molecules are quite frequent; mutual reactions among various reactive species occur easily; and physical effects such as UV radiation, cavitation effect, and supercritical oxidation can also participate in the generation of reactive species [8–12]. Thus, the energy yields for ·OH and H_2O_2 generation are usually higher than those in gas phase DBD plasma. Kirkpatrick and Locke studied the formation of H_2O_2 in a liquid pulsed discharge plasma system, and the energy yield for H_2O_2 generation was approximately 34.1 mmol l^{-1} kWh^{-1} [153]. Similar results were also observed by Lei *et al* [154], in whose research the energy yield for H_2O_2 generation in liquid pulsed discharge plasma was approximately 23.1 mmol l^{-1} kWh^{-1}. Bian *et al* [155] measured the formation of ·OH and H_2O_2 in a liquid pulsed discharge plasma, and the energy yields for ·OH and H_2O_2 generation were approximately 15.56 mmol l^{-1} kWh^{-1} and 224.2 mmol l^{-1} kWh^{-1}, respectively. Sahni and Locke [156] also reported that energy yields for ·OH and H_2O_2 generation were approximately 3.77 mmol l^{-1} kWh^{-1} and 34.3 mmol l^{-1} kWh^{-1} in a pulsed discharge system.

For gliding arc discharge plasma, the plasma is usually triggered in the gas phase, and the wastewater is located directly under the discharge plasma apparatus; some reactive species are first generated in the gas phase and then are pushed into the liquid phase by gas flow, and thus, similar to traditional gas phase DBD plasma, the energy yields for H_2O_2 and O_3 generation are usually low. Du *et al* [157] employed gas–liquid gliding arc discharge plasma to decolor acid orange wastewater, and the energy yields for H_2O_2 and O_3 generation were approximately 2.21 mmol l^{-1} kWh^{-1} and 0.016 mmol l^{-1} kWh^{-1}, respectively.

Glow discharge plasma is characterized as having high yields of ·OH and H_2O_2 that are much higher than those expected on the basis of Faraday's law. Depending on the trigger mode, glow discharge plasma contains contact glow discharge, DC diaphragm glow discharge, AC diaphragm glow discharge, etc. For contact glow discharge plasma, the plasma is triggered between the solution surface and the electrode in contact with it. Wang *et al* [158] studied the degradation of bisphenol A and formation of H_2O_2 in a contact glow discharge plasma system, and the energy yield for H_2O_2 generation was approximately

Table 3. Organic pollutants degradation in water in different discharge plasmas.

Discharge plasmas	Pollutants, removal efficiency	Conditions	Energy yield, G_{50} (g kWh^{-1})	References
AC DBD	Orange II, ~90%	In contact with liquid; 100 mg l^{-1}, 500 ml, 16.8 W, 23.3 kV	~4.5	[8]
AC DBD	Humic acid, ~90.9%	In contact with liquid; 30 mg l^{-1}, 500 ml, 50 Hz, 21.2 W, 19.6 kV	~2.08	[161]
AC DBD	Carbamazepine, ~90.7%	In contact with liquid; 20 mg l^{-1}, 100 ml, 12 W	~1.6	[162]
AC DBD	2,4-Ninitrophenol, ~95.0%	In contact with liquid; 100 mg l^{-1}, 500 ml, 40 W, 24 kV	~0.94	[152]
AC DBD	3,4-Dichloroaniline, ~96.1%	In contact with liquid; 16.2 mg l^{-1}, 100 ml, 135 W	~0.33	[163]
Pulsed DBD	Methyl red, ~93%	In contact with liquid; 10 mg l^{-1}, 200 ml, 76 Hz, 14 mJ pulse^{-1}	~0.94	[164]
Pulsed corona	Methyl orange, ~90%	In liquid; 40 mg l^{-1}, 100 ml, 7.1 W, 46 kV	~5.63	[141]
Pulsed corona	Phenol, ~98.1%	In liquid; 100 mg l^{-1}, 250 ml, 50 Hz, 21 kV	~2.71	[165]
Pulsed corona	4-Chlorophenol, ~95.7%	In liquid; 120 mg l^{-1}, 500 ml, 100 Hz, 16 kV	~2.66	[154]
Pulsed corona	Methyl orange, ~90%	In contact with liquid; 10 mg l^{-1}, 450 ml, 50 Hz, 22 kV	~0.45	[166]
Gliding arc	Acid orange 7, ~100%	In contact with liquid; 63 mg l^{-1}, 500 ml, 320 W	~0.12	[157]
Gliding arc	Bisphenol A, ~100%	In contact with liquid; 28 mg l^{-1}, 300 ml, 500 W	~0.08	[167]
Gliding arc	Forafac 1110, ~96.7%	In contact with liquid; 200 mg l^{-1}, 180 ml, 100 W	~0.64	[168]
Pulsed arc	4-Chlorophenol, ~35%	In liquid; 0.2 mmol l^{-1}, 1.0 l, 10.2 kV, 0.2 GW	~0.25	[169]
Glow discharge	Ionic liquids, ~90%	In liquid; 40 g l^{-1}, 100 ml, 600 V	~11.57	[170]
Glow discharge	Polar brilliant B, ~90%	In contact with liquid; 50 mg l^{-1}, 150 ml, 100 mA, 500 V	~0.16	[171]
Diaphragm glow discharge	Direct red 79, ~80%	In liquid; 30 mg l^{-1}, 3000 ml, 120 W	~0.61	[172]
MAP plasma jet	Methylene blue, ~98%	In contact with liquid; 2.45 GHz, 50 ml, 250 mg l^{-1}, 150 W	~0.296	[173]
AP plasma jet	Methylene blue, ~99%	In contact with liquid; 50 Hz, 50 ml, 30 mg l^{-1}, 5 W, 20 kV	~0.4	[174]

Note: AC, alternative current; DBD, dielectric barrier discharge; MAP, microwave atmospheric pressure; AP, atmospheric pressure.

411.8 mmol l^{-1} kWh^{-1}, which was much higher than that generated in DBD plasma, pulsed discharge plasma, and gliding arc discharge plasma. For diaphragm glow discharge plasma, DC and AC high voltage power supplies can both be used, and a diaphragm with a pin-hole is used to separate the cathode and anode electrodes; and the plasma is formed near the pin-hole. The H_2O_2 formation in a DC diaphragm glow discharge plasma system was studied by Wang [159], and the energy yield for H_2O_2 generation was approximately 96.0 mmol l^{-1} kWh^{-1}. In addition, the energy yield for H_2O_2 generation in an AC diaphragm glow discharge plasma system was approximately 168.3 mmol l^{-1} kWh^{-1}, as reported by Nikiforov and Leys [160].

As discussed above, the generation of reactive species is dependent on the discharge plasma type, and the energy yields for reactive species generation are also quite different, as shown in table 2, which may affect the organic pollutant degradation in different discharge plasmas. Energy yield is an important index to evaluate the possible application of discharge plasma in wastewater treatment. The energy yield (G_{50}) is defined as half of the target pollutant amount divided by the consumed energy. The energy yields for organic pollutant degradation in different discharge plasmas are listed in table 3. Here, AC DBD plasma, pulsed DBD, pulsed corona discharge, gliding arc discharge, pulsed arc discharge, glow discharge, microwave atmospheric pressure plasma jets, and atmospheric pressure plasma jets are compared in terms of pollutant removal efficiency, energy yield, and conditions [161–174]. The energy yields for pollutant removal using different discharge plasmas in contact with liquid are comparable (in most cases, $G_{50} < 1.0$ g kWh^{-1}); whereas much higher energy yields are obtained for pollutant removal using discharge plasmas in liquid than those in contact with liquid. For example, G_{50} values lower than 1.0 g kWh^{-1} are obtained for pulsed corona discharge in contact with liquid, while values of approximately 2.66–5.63 g kWh^{-1} are obtained for pulsed corona discharge in liquid [141, 154, 165, 166]; the same phenomenon is also observed for glow discharge plasma [170, 171]. These results suggest that the discharge plasma type and the contact method with liquid should be taken into consideration when discharge plasmas are used for wastewater treatment.

6. Future prospects and directions

Electrical discharge plasmas have generated considerable interest in wastewater treatment. The roles of various chemical and physical effects, including UV radiation, supercritical water oxidation, and oxidation by reactive species, have been discussed with respect to the various methods used for their measurement and their roles in the degradation of contaminants. The formation, reaction mechanisms, and mass transfer of these reactive species have also been analyzed. However, quantitative information is not available for some short-lived reactive species, and their contributions to wastewater treatment must be further evaluated. More research should be conducted to further discuss the feasibility of electrical discharge plasma for wastewater treatment and to develop effective ways to enhance the contaminant degradation efficiency.

At present, the combination of electrical discharge plasma with other processes, such as biological methods, activated carbon and nano-TiO_2, is considered as an effective approach to enhance the efficiency of discharge plasma in wastewater treatment [44, 175, 176]; in such cases, the electrical discharge plasma can act as a pretreatment method to first decompose the target contaminants into intermediates, which are more biodegradable or more likely to degrade or be removed via other low-energy processes.

Acknowledgments

The authors thank the Projects funded by National Natural Science Foundation of China (Nos. 51608448 and 21737003), Young Talent Cultivation Scheme Funding of Northwest A&F University (No. Z109021802), and the Fundamental Research Funds for the Central Universities (No. Z109021617) for their financial support in this research.

References

[1] Pradeep S *et al* 2013 *Biodegradation* **24** 257
[2] Pols H B and Harmsen G H 1994 *Water Sci. Technol.* **30** 109
[3] Zhang H *et al* 2011 *J. Hazard. Mater.* **190** 645
[4] Wang T *et al* 2015 *Sep. Purif. Technol.* **147** 17
[5] Wang T C *et al* 2016 *Environ. Sci. Pollut. Res.* **23** 13448
[6] Malik M A, Ghaffar A and Malik S A 2001 *Plasma Sources Sci. Technol.* **10** 82
[7] Lukes P *et al* 2005 *J. Phys. D: Appl. Phys.* **38** 409
[8] Mok Y S and Jo J O 2008 *Chem. Eng. J.* **14** 56
[9] Wang H J, Li J and Quan X 2006 *J. Electrost.* **64** 416
[10] Tang S F *et al* 2018 *Chem. Eng. J.* **337** 446
[11] Zhang R B *et al* 2003 *J. Dalian Univ. Technol.* **43** 719 (in Chinese)
[12] Shi H X *et al* 2005 *J. Environ. Sci.* **17** 926
[13] Sun Y H *et al* 2005 *J. Electrost.* **63** 969
[14] Sunka P 2001 *Phys. Plasmas* **8** 2587
[15] Grahl T and Maerkl H 1996 *Appl. Microbiol. Biotechnol.* **45** 148
[16] Schoenbach K H *et al* 2000 *IEEE Trans. Dielectr. Electr. Insul.* **7** 637
[17] Schoenbach K H *et al* 1997 *IEEE Trans. Plasma Sci.* **25** 284
[18] Sun B, Kunitomo S and Igarashi C 2006 *J. Phys. D Appl. Phys.* **39** 3814
[19] Sun B, Sato M and Clements J S 2000 *Environ. Sci. Technol.* **34** 509
[20] Mok Y S and Jo J O 2006 *IEEE Trans. Plasma Sci.* **34** 2624
[21] Locke B R *et al* 2006 *Ind. Eng. Chem. Res.* **45** 882
[22] Sunka P *et al* 2004 *Acta Phys. Slovaca* **54** 135
[23] Laroussi M and Leipold F 2004 *Int. J. Mass Spectrom.* **233** 81
[24] Bruggeman P J *et al* 2016 *Plasma Source Sci. Technol.* **25** 053002
[25] Robinson J W, Ham M and Balaster A N 1973 *J. Appl. Phys.* **44** 72
[26] Lukes P *et al* 2000 Role of various parameters on production of H_2O_2 by pulsed corona discharge in water *Proc. 6th Int. Conf. on Advanced Oxidation Technologies for Water and Air Remediation (London, Ontario, Canada, 26 June)*

[27] Matsumoto Y *et al* 1991 Inactivation of microorganisms by pulsed high voltage application *Conf. Record of IEEE Industrial Applications Society Annual Meeting* vol 1, pp 652
[28] Xue J, Chen L and Wang H L 2008 *Chem. Eng. J.* **138** 120
[29] Li J *et al* 2011 *Plasma Sources Sci. Technol.* **20** 034019
[30] Shih K Y and Locke B R 2010 *Plasma Chem. Plasma Process.* **30** 1
[31] Sugiarto A T *et al* 2003 *J. Electrost.* **58** 135
[32] Martin E A 1960 *J. Appl. Phys.* **31** 255
[33] Lu X, Pan T and Zhang H 2002 *Acta Phys. Sin.* **51** 1549
[34] Lu X *et al* 2001 *Explosion and Shockwaves* **21** 282
[35] Sunka P *et al* 2004 *IEEE Trans. Plasma Sci.* **32** 1609
[36] Gupta S B and Bluhm H 2008 *IEEE Trans. Plasma Sci.* **36** 1621
[37] Weaver J C and Chizmadzhev Y A 1996 *Bioelectrochem. Bioenerg.* **41** 135
[38] Fiala A *et al* 2001 *Innovative Food Sci. Emerg. Technol.* **2** 229
[39] Mizuno A and Hori Y 1988 *IEEE Trans. Ind. Appl.* **24** 387
[40] Hong K M and Noolandi J 1978 *J. Chem. Phys.* **69** 5026
[41] Kuskova N I 1983 *Sov. Phys. Technol. Phys.* **28** 591
[42] Wang T C *et al* 2018 *Chem. Eng. J.* **346** 65
[43] Joshi A A *et al* 1995 *J. Hazard. Mater.* **41** 3
[44] Wang H J *et al* 2008 *Appl. Catal.* B **83** 72
[45] Rumbach P *et al* 2015 *Nat. Commun.* **6** 7248
[46] Lukes P, Locke B R and Brisset J L 2012 Aqueous-phase chemistry of electrical discharge plasma in water and in gas–liquid environments *Plasma Chemistry and Catalysis in Gases and Liquids* (Hoboken, NJ: Wiley) pp 243–308
[47] Hoigné J 1997 *Water Sci. Technol.* **35** 1
[48] Dai Q Z, Lei L C and Zhang X W 2008 *Sep. Purif. Technol.* **61** 123
[49] Buxton G V *et al* 1988 *J. Phys. Chem. Ref. Data* **17** 513
[50] Gusten H *et al* 1995 *SAR QSAR Environ. Res.* **4** 197
[51] Benitez F J *et al* 2003 *Chemosphere* **51** 651
[52] Hong P K A and Zeng Y 2002 *Water Res.* **36** 4243
[53] Nemes A, Fabian I and Gordon G 2000 *Ozone Sci. Technol.* **22** 287
[54] Jiang N *et al* 2016 *Appl. Catal.* B **184** 355
[55] Zhao L *et al* 2009 *J. Hazard. Mater.* **161** 988
[56] Yang B, Zhou M H and Lei L C 2005 *Chemosphere* **60** 405
[57] Malic M A 2003 *Plasma Sources Sci. Technol.* **12** S26
[58] Hoigné J and Bader H 1976 *Water Res.* **10** 377
[59] Staehelin J and Hoigné J 1982 *Environ. Sci. Technol.* **16** 676
[60] Hoigné J 1998 Chemistry of aqueous ozone and transformation of pollutants by ozonation and advanced oxidation processes *Quality and Treatment of Drinking Water II* (Berlin: Springer) pp 83–141
[61] Zhang J *et al* 2003 *Res. Chem. Intermed.* **29** 839
[62] Zhang J B *et al* 2008 *J. Hazard. Mater.* **154** 506
[63] Jamroz P *et al* 2018 *Plasma Process Polym.* **15** 1700083
[64] Wang T C *et al* 2011 *Environ. Sci. Technol.* **45** 9301
[65] Szabó-Bárdos E *et al* 2011 *Appl. Catal.* B **101** 471
[66] Wang T C *et al* 2014 *Plasma Chem. Plasma Process.* **34** 1115
[67] Hao X L, Zhang X W and Lei L C 2009 *Carbon* **47** 153
[68] Kabakchi S A, Kartasheva L I and Lebedeva I E 1988 *Int. J. Radiat. Appl. Instrum.* A **32** 541
[69] Jamróz P *et al* 2014 *Plasma Chem. Plasma Process.* **34** 25
[70] Chavadej S, Saktrakool K and Rangsunvigit P 2007 *Chem. Eng. J.* **132** 345
[71] Fancey K S 1995 *Vacuum* **46** 695
[72] Zhang Y *et al* 2007 *Chemosphere* **67** 702
[73] Mills A and LeHunte S 1997 *J. Photochem. Photobiol.* A **108** 1
[74] Simek M and Clupek M 2002 *J. Phys. D: Appl. Phys.* **351** 171
[75] Ghezzar M R *et al* 2008 *Appl. Catal.* B **72** 304
[76] Ikawa S, Kitano K and Hamaguchi S 2010 *Plasma Process. Polym.* **7** 33
[77] Thomas J K *et al* 1966 *J. Phys. Chem.* **70** 2409
[78] Marklund S 1976 *J. Biol. Chem.* **251** 7504
[79] Perni S *et al* 2007 *Appl. Phys. Lett.* **90** 073902
[80] Korshunov S S and Imlay J A 2002 *Mol. Microbiol.* **43** 95
[81] Jiang B *et al* 2014 *Chem. Eng. J.* **236** 348
[82] Lecuiller M, Julien R and Pucheault J 1972 *J. Chim. Phys.* **69** 1353
[83] Goldman A *et al* 1992 *Pure Appl. Chem.* **64** 759
[84] Grymonpre D R *et al* 2001 *Chem. Eng. J.* **82** 189
[85] Lukes P *et al* 2008 *Plasma Sources Sci. Technol.* **17** 024012
[86] Mededovic S and Locke B R 2007 *Appl. Catal.* B **72** 342
[87] Sun B, Sato M and Clements J S 1997 *J. Electrost.* **39** 189
[88] Hayashi D *et al* 2000 *J. Phys. D: Appl. Phys.* **33** 2769
[89] Doubla A *et al* 2003 *J. Appl. Electrochem.* **33** 73
[90] Gupta S B 2007 Investigation of a physical disinfection process based on pulsed underwater corona discharge *PhD* Karlsruhe Institute of Technology, Forschungszentrum Karlsruhe, Germany
[91] Selles R M 1980 *Analyst* **105** 950
[92] Wang H J *et al* 2007 *J. Hazard. Mater.* **14** 336
[93] Yan J H *et al* 2005 *Plasma Sources Sci. Technol.* **14** 1
[94] Qu G Z *et al* 2013 *Chem. Eng. J.* **228** 28
[95] Hsieh K, Wang H J and Locke B R 2016 *J. Hazard. Mater.* **317** 188
[96] Porter D *et al* 2009 *IEEE Trans. Ind. Appl.* **45** 623
[97] Sarasa J *et al* 2002 *Water Res.* **36** 3035
[98] Pawlat J *et al* 2002 *Ozone Sci. Technol.* **24** 181
[99] Ryu S and Park H 2009 *J. Electrost.* **67** 723
[100] Wang T C *et al* 2014 *J. Hazard. Mater.* **264** 169
[101] Ihara S *et al* 1999 *Japan. J. Appl. Phys.* **38** 4601
[102] Ono R and Oda T 2007 *J. Phys. D: Appl. Phys.* **40** 176
[103] Ono R and Oda T 2003 *J. Appl. Phys.* **93** 5876
[104] Ono R and Oda T 2004 *J. Phys. D: Appl. Phys.* **37** 730
[105] Wang T C *et al* 2016 *J. Hazard. Mater.* **302** 65
[106] Wu J L *et al* 2007 *J. Northwest Normal Univ.* **43** 53
[107] Bian W J, Zhou M H and Lei L C 2007 *Plasma Chem. Plasma Process.* **27** 337
[108] Tai C *et al* 2004 *Anal. Chim. Acta* **527** 73
[109] Harbour J R, Chow V and Bolton J R 1974 *Can. J. Chem.* **52** 3549
[110] Finkelstein E, Rosen G M and Rauckman E J 1980 *Arch. Biochem. Biophys.* **200** 1
[111] Kanazawa S *et al* 2011 *Plasma Sources Sci. Technol.* **20** 034010
[112] Du Y J *et al* 2017 *Plasma Sources Sci. Technol.* **26** 095007
[113] Sun M and Cai L J 2012 *IEEE Trans. Plasma Sci.* **40** 1395
[114] Liu F *et al* 2008 *Spectrochim. Acta* A **69** 776
[115] Wang H J *et al* 2007 *Spectrosc. Spect. Anal* **27** 2506
[116] Mok Y S *et al* 2002 *IEEE Trans. Plasma Sci.* **30** 408
[117] Ono R and Oda T 2000 *IEEE Trans. Ind. Appl.* **36** 82
[118] Lowke J J and Morrow R 1995 *IEEE Trans. Plasma Sci.* **23** 661
[119] Ono R and Oda T 2001 *IEEE Trans. Ind. Appl.* **37** 709
[120] Sankaranarayanan R, Pashaie B and Dhali S K 2000 *Appl. Phys. Lett.* **77** 2970
[121] Kanazawa S *et al* 2007 *Thin Solid Films* **515** 4266
[122] Nikiforov A *et al* 2011 *Eur. Phys. J. Appl. Phys.* **56** 24009
[123] Katayama H *et al* 2009 *IEEE Trans. Plasma Sci.* **37** 897
[124] Nikiforov A *et al* 2011 *Appl. Phys. Express* **4** 026102
[125] Bielskie B H J *et al* 1985 *J. Phys. Chem. Ref. Data* **14** 1041
[126] Sahni M and Locke B R 2006 *Plasma Process Polym.* **3** 342
[127] Sato M, Ohgiyama T and Clements J S 1996 *IEEE Trans. Ind. Appl.* **32** 106
[128] Locke B R and Thagard S M 2012 *Plasma Chem. Plasma Process.* **32** 875
[129] Karpel Vel Leitner N *et al* 2005 *Water Res.* **39** 4705
[130] Zhang H *et al* 2012 *Water Res.* **46** 6554
[131] Wang T C *et al* 2015 *Water Res.* **84** 18

[132] Gorman A A and Rodgers M A J 1981 *Chem. Soc. Rev.* **10** 205
[133] Zhang D D *et al* 2009 *J. Hazard. Mater.* **163** 843
[134] Ono R and Oda T 2009 *Plasma Sources Sci. Technol.* **18** 035006
[135] Ono R, Teramoto Y and Oda T 2010 *Plasma Sources Sci. Technol.* **19** 015009
[136] Hong Y *et al* 2013 *IEEE Trans. Plasma Sci.* **41** 545
[137] Chang C H and Franses E I 1995 *Colloids Surf.* A **100** 1
[138] Minagawa Y *et al* 2014 *Japan. J. Appl. Phys.* **53** 010210
[139] Cserfalvi T and Mezei P 1996 *Fresenius J. Anal. Chem.* **355** 813
[140] Norberg S A *et al* 2014 *J. Phys. D: Appl. Phys.* **47** 47503
[141] Zhang Y Z *et al* 2008 *Chemosphere* **70** 1518
[142] Tsouris C *et al* 1995 *Ind. Eng. Chem. Res.* **34** 1394
[143] Tsouris C, Shin W T and Yiacoumi S 1998 *Can. J. Chem. Eng.* **76** 589
[144] Chu L B *et al* 2007 *Chemosphere* **68** 1854
[145] Zieminski S A, Caron M M and Blackmore R B 1967 *Ind. Eng. Chem. Fundam.* **6** 233
[146] Cheng J 1995 The research on ozonation of p-nitroaniline aqueous solution and mass transfer model *PhD Thesis* South China University of Technology, Guangzhou, China (in Chinese)
[147] Ren J Y *et al* 2015 *Plasma Sci. Technol.* **17** 1
[148] Iseni S *et al* 2014 *J. Phys. D: Appl. Phys.* **47** 152001
[149] Robert E *et al* 2014 *Plasma Source Sci. Technol.* **23** 012003
[150] Shimizu T *et al* 2011 *New J. Phys.* **13** 053025
[151] Burlica R, Kirkpatrick M J and Locke B R 2006 *J. Electrost.* **64** 35
[152] Tang Q *et al* 2009 *Chem. Eng. J.* **153** 94
[153] Kirkpatrick M J and Locke B R 2006 *Ind. Eng. Chem. Res.* **45** 2138
[154] Lei L C *et al* 2007 *Ind. Eng. Chem. Res.* **46** 5469
[155] Bian W J, Ying X L and Shi J W 2008 *J. Hazard. Mater.* **162** 906
[156] Sahni M and Locke B R 2006 *Ind. Eng. Chem. Res.* **45** 5819
[157] Du C M *et al* 2008 *J. Hazard. Mater.* **154** 1192
[158] Wang L, Jiang X Z and Liu Y J 2007 *J. Hazard. Mater.* **154** 1106
[159] Wang L 2009 *Plasma Chem. Plasma Process.* **29** 241
[160] Nikiforov A Y and Leys C 2007 *Plasma Sources Sci. Technol.* **16** 273
[161] Wang T C *et al* 2016 *Water Res.* **89** 28
[162] Liu Y N *et al* 2012 *Chem. Eng. Process.* **56** 10
[163] Feng J W *et al* 2015 *Environ. Sci. Pollut. Res.* **22** 4447
[164] Piroi D *et al* 2010 Pulsed dielectric barrier discharge generated at the gas liquid interface for the degradation of the organic dye methyl red in aqueous solution *12th Int. Conf. Optim. Electri. Electron. Equip. (Brasov, Romania)*
[165] Wang H J and Chen X Y 2011 *J. Hazard. Mater.* **186** 1888
[166] Sun B *et al* 2012 *J. Environ. Sci.* **24** 840
[167] Abdelmalek F *et al* 2008 *Sep. Purif. Technol.* **63** 30
[168] Marouf-Khelifa K *et al* 2008 *Chemosphere* **70** 1995
[169] Willberg D M and Lang P S 1996 *Environ. Sci. Technol.* **30** 2526
[170] Gao J *et al* 2014 *J. Hazard. Mater.* **265** 261
[171] Wang L 2009 *J. Hazard. Mater.* **171** 577
[172] Stará Z *et al* 2009 *Desalination* **239** 283
[173] Garcia M C *et al* 2017 *Chemosphere* **180** 239
[174] Chandana L, Manoj Kumar Reddy P and Subrahmanyam C 2015 *Chem. Eng. J.* **282** 116
[175] Grymonpre D R *et al* 2003 *Ind. Eng. Chem. Res.* **42** 5117
[176] Tang S F *et al* 2013 *Carbon* **53** 380